TITLE

Optimized CRISPR inhibition and activation opens key avenues for systematic biological exploration in zebrafish.

AUTHORS

Nelson B. Barrientos[1], Elyse A. Shoppell[1], Rachel J. Boyd[1], Valeria C. Culotta[2], Andrew S. McCallion[1,3*]

AFFILIATIONS

[1]McKusick-Nathans Department of Genetic Medicine, Johns Hopkins University School of Medicine, Baltimore, MD 21205, USA

[2]Department of Biochemistry and Molecular Biology, Johns Hopkins University Bloomberg School of Public Health, Baltimore, MD 21205, USA

[3]Department of Medicine, Johns Hopkins University School of Medicine, Baltimore, MD 21205, USA

[*] Corresponding author

ABSTRACT

The application of CRISPR interference (CRISPRi) and CRISPR activation (CRISPRa) technologies in zebrafish has the potential to expand its capacity for the study of gene function significantly. We have developed a codon optimized CRISPRi/a for zebrafish; here we provide proof-of-principle data across established pigmentary and growth phenotypes. We established a zebrafish codon-optimized *cas9* gene, harboring mutations D10A and D839A to render the protein catalytically inactive (*dCas9*). Similarly, codon-optimized Krüppel associated box (KRAB) and methylated CP2 (MeCP2) inactivating domains or VP64 activator domain were cloned downstream from *dCas9* for CRISPRi and CRISPRa, respectively. To validate CRISPRi, we targeted key genes in melanocyte differentiation (*sox10, mitfa,* and *mitfb)*; and melanin production (tyrosinase; *tyr*). Microinjection of CRISPRi mRNA and single guide RNAs (sgRNAs) targeting the *tyr* promoter or 5'-UTR resulted in larvae with hypopigmented epidermal melanocytes. Transcription factors mitfa and mitfb similarly direct differentiation and pigmentation of epidermal melanocytes (*mitfa*) and retinal pigment epithelium (RPE, *mitfb*). CRISPRi-mediated targeting of their promoters or 5'-UTR also results in pronounced hypopigmentation of epidermal melanocytes (*mitfa*), and RPE (*mitfb*). So too, targeting CRISPRi to the *sox10* promoter results in hypopigmentation of both epidermal melanocytes and RPE consistent with its role upstream of *mitfa* and *mitfb*, and *tyr*. Finally, we asked whether CRISPRi and CRISPRa could be used to modulate a single gene, to yield hypomorphic and hypermorphic effects, selecting *mrap2a*, as our target. This gene regulates energy homeostasis and somatic growth via inhibition of the melanocortin 4 receptor gene (*mc4r*). We demonstrate that targeting the *mrap2a* 5'-UTR with CRISPRa or CRISPRi significantly increases or decreases larval body length, respectively. We demonstrate the utility of CRISPRi/a for modulating control of zebrafish gene expression, facilitating efficient assay of candidate gene function and disease relevance.

KEYWORDS:

Zebrafish, CRISPR-activation, CRISPR-inhibition

INTRODUCTION

Zebrafish (*danio rerio*) are a powerful model system in which to study functional components of vertebrate genomes. Comparative genomics analyses have shown that 61.5% of mouse protein-coding genes and 71% of human protein-coding genes have at least one zebrafish orthologue[1,2]. Additional features, including short generation time, high fecundity, external fertilization, and embryonic transparency, have distinguished zebrafish as a desirable model system in which to examine developmental processes. As such, zebrafish have been widely used to study the biological relevance of regulatory elements[3–6], and human disease-associated genes[7–14].

Emerging technologies for transgenesis and genome engineering, such as such as Gal4-UAS[15]; Tol2-transposase transgenesis[3]; Zinc Finger Nucleases[16]; and transcription activator-like effectors (TALENs)[17] have been developed and rapidly implemented in zebrafish. Over the last decade, zebrafish have also been shown to be amenable to CRISPR-Cas-based genomic engineering applications, including targeted mutagenesis, base editing, and generation of knock-in and knockout models[18–22]. More recently, the emergence of CRISPR interference (CRISPRi) and activation (CRISPRa) have presented additional opportunities to explore functional components of vertebrate genomes. CRISPRi/a involves the fusion of transcriptional effectors to a catalytically inactive, or “dead” Cas9 (dCas9). CRISPRi employs a transcriptional repressor, such as a Krüppel associated box (KRAB) domain and methyl-CpG binding protein 2 (MeCP2)[23,24], while in the case of CRISPRa, a transcriptional activator, such as VP64, is fused to the dCas9[25]. To date, the CRISPRi/a systems have seen limited application in zebrafish[26],

76 whereas they have been more rapidly employed in mammalian organisms to target human
77 disease-relevant genes[27–29].

78 Here, we report initial experiments in the development and evaluation of zebrafish codon-
79 optimized zdCas9-KRAB-MeCP2 and zdCas9-VP64 CRISPR systems. We present a systematic
80 evaluation of these modified proteins in functional proof-of-concept experiments by targeting two
81 easily scored phenotypes: zebrafish pigmentation and somatic growth. In addition to providing
82 visual confirmation of the efficacy of both CRISPRi and CRISPRa, these two model phenotypes
83 and their corresponding pathways are well-characterized and are involved in human disease.

84 Specifically, we chose to test our CRISPRi system by targeting genes involved in
85 melanocyte differentiation and pigmentation, *sox10 (SRY-box transcription factor 10)*, *mitfa*
86 *(melanocyte inducing transcription factor a)*, *mitfb*; and the gene for the rate determining enzyme
87 in pigmentation, *tyr (tyrosinase)*. At approximately 16 hours post fertilization (16 hpf), *sox10*
88 directly activates *mitfa* and *mitfb* promoters to stimulate downstream genes involved in
89 melanocyte differentiation; and activates *tyr*, to induce melanin production by 24 hpf[30–32]. In the
90 developing zebrafish embryo, *mitfa* and *mitfb* are co-expressed in the retinal pigment epithelium,
91 whereas only *mitfb* is expressed in the zebrafish epiphysis and olfactory bulb, and only *mitfa* is
92 expressed in neural crest cells[31,33,34]. We hypothesize that independently targeting each of these
93 four genes with functional CRISPRi will yield a visible reduction in zebrafish pigmentation. In the
94 case of *sox10,* we expect to see marked reduction in pigmentation globally due to its role in
95 melanocyte cell fate and activation of *mitfa/b* and *tyr* to promote melanin production in zebrafish
96 and other vertebrates[35,36]. Due to its role in multiple stages of melanocyte differentiation and its
97 function as a transcription factor, silencing *mitfa* is expected to result in a hypopigmentation
98 phenotype throughout the body[37]. Similarly, silencing *mitfb* is expected to delay melanocyte
99 differentiation in the retinal pigment epithelium (RPE) and lead to areas of reduced
100 pigmentation[33,38]. Lastly, we hypothesize that targeting *tyr* will result in hypopigmentation of
101 melanocytes throughout the zebrafish body[30,35,39,40]. Zebrafish melanocytes have been

102 extensively studied by our group and others[4,6,41,42], and targeting genes in this pathway is highly
103 relevant to the study of human disease, including melanoma[43–45], Waardenburg Syndrome[46,47],
104 microphthalmia, and Hirschsprung's disease[48,49].

105 For our CRISPRa system, we chose to target *mrap2a* (*melanocortin receptor accessory*
106 *protein 2a*), which has been found to inhibit the transcription of the *melanocortin-4 receptor*
107 (*mc4r*)[50]. As a corollary, we hypothesize that CRISPRa targeting the *mrap2a* locus will amplify the
108 inhibition of *mc4r* and promote visible growth phenotypes in zebrafish larvae. This is supported
109 by evidence in human patients, wherein autosomal dominant loss of function mutations in *MCR4*
110 results in severe childhood-onset obesity[51,52]. By contrast, we hypothesize that effective CRISPRi
111 targeting of *mrap2a* will promote *mc4r* inhibition and result in diminished zebrafish growth similar
112 to previous knock-down experiments using morpholinos[50].

113 Ultimately, we outline the development of zebrafish-optimized zdCas9-KRAB-MeCP2 and
114 zdCas9-VP64 CRISPR constructs. We establish their utility for efficient screening of candidate
115 gene function and disease relevance. Ongoing work in the lab will establish stable transgenic
116 lines expressing these proteins to facilitate rapid and systematic screening of gain and loss of
117 gene function targeting custom guide RNAs (gRNAs) to promoters, 5'-UTR, or cell-dependent cis-
118 regulatory elements of selected candidate genes.

119

120 METHODS

121

122 **Generation of catalytically inactive Cas9 plasmid vector**

123 The WT zebrafish optimized Cas9 within the plasmid vector pT3TS-nCas9n (Addgene
124 #46757) was mutated to produce a catalytically inactive dead Cas9 (dCas9). The DNA sequence
125 corresponding to the RuvC-like and HNH nuclease domains of the Cas9 protein were modified
126 by inducing a change from Aspartic acid to Alanine at position 10 (D10A), and a change from

127 Histidine to Alanine at position 839 (H839A). This was accomplished by implementing the
128 NEBuilder HiFi DNA Assembly (Cat. # E5520S) protocol using oligonucleotides primers
129 (Supplemental Table 1) generated using the NEBuilder Assembly Tool (v.2.10.1). The modified
130 plasmid vector was then transformed into NEB 5-a competent *E. coli* cells (Cat. # C2987I) and
131 later mini-prepped using NEB Monarch Plasmid Miniprep Kit (Cat. # T1010L). The plasmid vector
132 generated was named pT3TS-ndCas9n.
133
134 **Codon Optimization of KRAB-MeCP2 and VP64 domains for zebrafish usage**
135 The DNA sequence for the KRAB-MeCP2 repressor was obtained from the dCas9-KRAB-
136 MeCP2 plasmid vector (Addgene #110821); while the DNA sequence for the VP64 activator was
137 obtained from the dCas9-VP64-GFP plasmid vector (Addgene #61422). The codon optimization
138 tool from IDT was used to optimize these sequences for zebrafish. The KRAB-MeCP2 repressor
139 sequence (1,263 bp) containing an SV40 NLS before and after KRAB was optimized and ordered
140 as a gBlocks HiFi Gene Fragment. The VP64 activator sequence (225 bp) containing an SV40
141 NLS before VP64 was optimized and ordered as a gBlocks Gene Fragment.
142
143 **CRISPRi/a plasmid construct generation and *in vitro* transcription**
144 The codon optimized KRAB-MeCP2 repressor and VP64 activator were cloned into the
145 pT3TS-ndCas9n plasmid vector containing a catalytically inactive dCas9 sequence. Cloning was
146 carried out by employing NEBuilder HiFi DNA Assembly (Cat. # E5520S) using oligonucleotide
147 primers (Supplemental Table 2) that overlapped both the target region of the plasmid vector and
148 the optimized sequences. Once the optimized sequences had been cloned in, the plasmid
149 constructs were transformed into NEB 5-a competent *E. coli* cells (Cat. # C2987I) and later mini-
150 prepped using NEB Monarch Plasmid Miniprep Kit (Cat. # T1010L). The plasmid constructs
151 generated were named zdCas9-KRAB-MeCP2 and zdCas9-VP64 for CRISPRi and CRISPRa,
152 respectively.

153 The restriction enzyme XbaI (NEB Cat # R0145) was used to linearize the CRISPRi/a
154 plasmid constructs. Subsequently, *in vitro* transcription of the d*Cas9* gene plus the repressor or
155 activator was performed by employing the mMessage mMachine T3 Transcription kit (Cat. #
156 AM1348). RNA was recovered by using the RNA Clean-up protocol from the Qiagen RNeasy Mini
157 Kit (Cat. # 74104) and stored at -80°C.
158

159 **Designing targeted gRNAs for CRISPRi/a**

160 Multiple single guide RNAs (sgRNAs) were designed to target the promoter or 5'-UTR of
161 the various genes in the zebrafish. All sgRNAs followed a core **5'-N18-3'**[53] sequence and were
162 designed using the online tool CRISPOR (PMID: 29762716). At the 5' end of the forward
163 oligonucleotide, the nucleotides 5'-TAGG-3' were added. At the 5' end of the reverse
164 oligonucleotide (reverse complement of N18 sequence), the nucleotides 5'-AAAC-3' were added.
165 The final form of the oligonucleotides was 5'-TAGG-N18-3' for the forward oligo; and 5'-AAAC-
166 N18RevCompl-3'. The oligo primers for each sgRNA were ordered from IDT (Supplemental Table
167 3). Oligonucleotide primers were first annealed and subsequently cloned into the pT7-gRNA
168 plasmid vector (Addgene #46759) containing a gRNA scaffold, according to restriction enzyme
169 cloning protocol specifications from previous studies[54]. After cloning, each plasmid construct
170 generated for each sgRNA was transformed into NEB 5-a competent *E. coli* cells (Cat. # C2987I)
171 and later mini-prepped using NEB Monarch Plasmid Miniprep Kit (Cat. # T1010L). Linearization
172 of these constructs was performed using the restriction enzyme BamHI-HF (NEB Cat # R3136).
173 The linear DNA was purified using the Zymo Research DNA Clean & Concentrator-5 protocol
174 (Cat. # D4013). Subsequently, *in vitro* transcription of linear DNA was performed using the
175 Thermo Fisher MEGAshortscript T7 Kit (Cat. # AM1354) or the NEB HiScribe T7 High Yield RNA
176 Synthesis Kit (Cat. #E2040S). After in vitro transcription, RNA was recovered by using the RNA
177 Clean-up protocol from the Qiagen RNeasy Mini Kit (Cat. # 74104) and stored at -80°C.
178

179 **Zebrafish husbandry and microinjections of one-cell stage embryos**

180 The day before injections, adult AB zebrafish (ZFIN ID: ZDB-GENO-960809-7) crosses
181 were set up in tanks with dividers at a ratio of 2:1 or 3:2 females per male. The morning of
182 injections and when the lights came on, the dividers were removed to allow for mating among
183 zebrafish. Zebrafish embryos were injected during the first 15-20 mins after being collected to
184 ensure injection occurred at the one-cell stage. The mixture injected to the embryos contain 300
185 ng of CRISPRi/a mRNA, 150 ng of sgRNA mRNA, 0.5 µl of Phenol Red, and Nuclease Free Water
186 up to 6 µl. After microinjections, zebrafish embryos were incubated at 28 °C in E3 embryo medium
187 provided by Johns Hopkins FinZ Zebrafish Core Center.

188

189 **Zebrafish measurement and image collection**

190 All zebrafish larvae used for measurements or image collection at 48 hpf or later were first
191 anesthetized using ethyl-3-aminobenzoate methanesulfonate salt (Tricane/MS-222; Sigma
192 Aldrich #E10521) prepared at a concentration of 4 mg/mL using 1 M Tris (pH 9, 4% v/v). The
193 Nikon AZ100 Multizoom fluorescent microscope was used for both measurements and image
194 collection at a ratio of 3.22 µm/px. For all images, zebrafish larvae were suspended in 3% Methyl
195 Cellulose (Sigma Aldrich #M0387) solution.

196 RESULTS

197

198 **CRISPRi modulates tyrosinase expression up to 48 hours post fertilization.**

199 To determine the functional capacity of zebrafish codon-optimized CRISPRi (Fig 1A), one-
200 cell stage zebrafish embryos were injected with CRISPRi mRNA and target sgRNAs. A CRISPRi
201 assay for zebrafish provides an opportunity to ask questions regarding the impact of titrating
202 downwards the expression of target genes, in evaluation of their normal biological role. As part of
203 a series of proof-of-concept experiments, we designed sgRNAs targeting the promoter region and

204 5'-UTR of the tyrosinase (*tyr*) gene, predicting that inhibition would lead to diminished larval
205 pigmentation, similar to established loss of function studies at this locus[30,32,40].

206 Initially, sgRNAs were designed to target the *tyr* promoter or 5'-UTR (Methods) and one-
207 cell embryos (n ≥ 200) were injected with CRISPRi (300 ng/µl) and a cocktail of all five sgRNAs
208 (150 ng/each). Zebrafish larvae assayed at 48 hpf displayed marked reduction in pigmentation of
209 melanocytes (Fig 1B), consistent with phenotypes arising from loss of function alleles in
210 zebrafish[30] and other vertebrates[39]. By contrast, larvae receiving only the CRISPRi mRNA (n ≥
211 200) or uninjected controls (n ≥ 200), displayed no diminution in melanization at 48 hpf. As
212 expected, the observed suppression of tyr dissipated over time, and by 72 hpf melanization was
213 indistinguishable between controls and those larvae receiving CRISPRi and the cocktail of all
214 sgRNAs.

215 We next tested if delivery of each individual *tyr* sgRNAs could similarly silence
216 transcription of *tyr* and reduce melanin production. At least one of the five sgRNAs that we tested,
217 sgRNA4 targeting the promoter, efficiently modulated *tyr* expression (Supp Fig 1), resulting in
218 hypopigmentation at 48 hpf. We used this sgRNA to assess the optimal concentration of sgRNA
219 and injected n ≥ 200 larvae each with 100 ng/µl, 300 ng/µl, and 500 ng/µl of sgRNA4. Our data
220 suggests no advantage to injection of levels in excess of 300 ng/µl of sgRNA (Supp Fig 1).

221 These results demonstrate the effectiveness in modulating *tyr* by employ of our zebrafish
222 codon-optimized CRISPRi and selected individual or pooled sgRNA targeting the gene's
223 promoter. To build on these observations, we sought to confirm them through the manipulation of
224 other key pigment genes that are known to regulate *tyr*.

225

226 **CRISPRi modulates melanin production upon targeting of *mitf* genes.**

227 In light of our results modulating *tyr* expression, we next tested if we could induce its
228 silencing by targeting the genes encoding the transcription factors mitfa and mitfb. The *mitf* genes
229 play critical roles in pigmentation throughout vertebrates, targeting tyrosinase during early

230 development[35,55]. We designed sgRNAs to target the promoter and 5'-UTR regions of the *mitfa*
231 and *mitfb* genes, predicting that, as with known loss-of-function (LoF) alleles[34,55], titrating activity
232 of these transcriptions factors would result in reduced activation of tyrosinase in melanocytes
233 throughout the body (*mitfa*) and in the retinal pigment epithelium (*mitfa* and *mitfb*).

234 Four sgRNAs were designed to target the *mitfa* promoter (Methods). As before, zebrafish
235 one-cell embryos (n ≥ 200) injected with CRISPRi (300 ng/µl) and a cocktail of all *mitfa* sgRNAs
236 (150 ng/each) displayed marked reduction in pigmentation of melanocytes, assayed at 48 hpf (Fig
237 2a). This is consistent with prior *mitfa* LoF studies[56] where failure to express *mitfa* prevents the
238 production of melanocyte precursors, leading to reduced global pigmentation in zebrafish larvae.
239 In contrast, no reduction in pigmentation was observed in larvae receiving only the CRISPRi
240 mRNA (n ≥ 200) or uninjected controls (n ≥ 200) (Fig 2A). Additionally, individual *mitfa* sgRNAs
241 targeting the promoter or 5'-UTR effectively silenced *mitfa,* resulting in marked reduction of
242 melanin production at 48 hpf (Supp Fig 2). Silencing of *mitfa* dissipated over time and at
243 approximately 72 hpf, melanization was similar between controls and injected larvae (Fig 2A,
244 Supp Fig 2A).

245 For *mitfb,* five sgRNAs were designed to target the promoter and 5'-UTR (Methods), and
246 one-cell zebrafish larvae (n ≥ 200) were injected with CRISPRi (300 ng/µl) with or without a
247 cocktail of all *mitfb* sgRNAs (150 ng/each). Injected larvae were assayed at 48 and 72 hpf for
248 differences in melanization in the RPE, and compared with uninjected controls (n ≥ 200) at the
249 same developmental time. RPE morphogenesis starts at around 16 hpf and by 27 hpf, a single
250 monolayer RPE has formed and pigmentation is initiated[57]. At 48 hpf, although control larvae did
251 not show a fully pigmented RPE, larvae injected with CRISPRi and gRNAs showed a noticeable
252 hypopigmentation phenotype (Fig 2b). When these larvae were assayed at 72 hpf, pigmentation
253 patterns in control conditions showed a fully pigmented RPE. By contrast, injected larvae showed
254 a pigmentation pattern in the form of patches of diminished pigmentation (Fig 2b). Prior *mitfb* LoF
255 studies have indicated that a combination of *mitfa, mitfb* and the *otx* genes is necessary for proper

256 development of the RPE in zebrafish[33]. Therefore, silencing *mitfb* likely delays RPE pigmentation
257 as a consequence of delaying its development. Furthermore, individual *mitfb* sgRNAs, whether
258 they targeted the promoter or 5'-UTR, were capable of modulating *mitfb* expression and resulted
259 in patches of reduced pigmentation in the RPE (Supp Fig 3A). However, the level of modulation
260 induced by each sgRNA differed as some of them were presented with hypopigmented patches
261 as early at 48 hpf and their effect was still noticeable at 72 hpf (Supp Fig 3A). By contrast, other
262 sgRNAs were able to modulate *mitfb* by 48 hpf but their effect had dissipated by 72 hpf (Supp Fig
263 3A), confirming the transient effect of our CRISPRi system.

264 These results imply that our zebrafish codon-optimized CRISPRi is effective at modulating
265 expression of the *mitf* genes, which results in indirect modulation of *tyr* gene expression amongst
266 other genes, leading to melanocyte hypopigmentation.

267

268 **CRISPRi targeting of transcription factor *sox10* silences pigmentation pathway in**
269 **zebrafish**

270 Having established that *tyr*, and *mitfa/b* can be modulated via CRISPRi, we sought to
271 move our assays upstream of these factors, investigating whether *sox10*, a transcription factor
272 known to activate *mitfa/b* and to promote melanin production in zebrafish and other
273 vertebrates[35,36]. We designed sgRNAs to target the promoter of the *sox10* gene, predicting that
274 silencing it would lead to downregulation of *mitfa/b* and *tyr* and subsequent hypopigmentation in
275 the zebrafish.

276 Four gRNAs were designed to target the *sox10* promoter (Methods). Zebrafish larvae (n
277 ≥ 200) injected with CRISPRi (300 ng/µl) and a cocktail of all *sox10* sgRNAs (150 ng/each)
278 displayed marked reduction in pigmentation of melanocytes, assayed at 48 hpf, consistent with
279 reduction of pigmentation when targeting downstream genes *mitfa/b,* and *tyr* (Fig 3A, Supp Fig
280 4A). Consistent with our results, no reduction in pigmentation was observed in larvae receiving
281 only the CRISPRi mRNA (n ≥ 200) or uninjected controls (n ≥ 200) (Fig 3A). Furthermore, we

282 observed that at least one sgRNAs (Fig 3A, 3B, Supp Fig 4A) was effective at reducing
283 pigmentation when injected individually. These results are in line with previous work that
284 demonstrated that *sox10* is important for melanocyte development and melanin production[35,36,58].
285 The effects of CRISPRi dissipated by 72 hpf as the pigmentation patterns between injected and
286 uninjected were indistinguishable (Fig 3A).

287 Because *sox10* also targets *mitfb* for activation, we investigated if silencing *sox10* would
288 have any effect on the RPE. We observed that silencing *sox10* leads to delay in pigmentation in
289 the RPE (Fig 3B). Consistent with our results, at 48 hpf, the RPE is not fully pigmented and no
290 differences are observed between controls and experimental conditions (Supp Fig 4A). At 72 hpf,
291 different pigmentation patterns in the form of patches of reduced pigmentation between conditions
292 were observed ventrally in injected larvae (Fig 3B). This is similar to the phenotype observed
293 when targeting *mitfb*, suggesting that silencing *sox10* leads to reduced transcription of *mitfb,*
294 which leads to subsequent delay in RPE development and pigmentation. By contrast, the RPE in
295 controls was fully pigmented at 72 hpf (Fig 3B).

296 These results imply that our zebrafish codon-optimized CRISPRi is effective at modulating
297 the expression of any particular gene and the effect of silencing any gene leads to downregulation
298 of downstream genes.

299

300 **CRISPRi/a affects zebrafish length by modulating transcription of *mrap2a***

301 In light of being able to modulate zebrafish pigmentation using our CRISPRi system, we
302 wanted to test our CRISPRa system by modulating a more applicable phenotype. We targeted
303 the *mrap2a* gene which is known to regulate the expression of the melanocortin 4 receptor (*mc4r*)
304 gene by silencing its transcription[50,59]. Both of these genes have been shown to be involved in
305 energy homeostasis and somatic growth in mice and zebrafish, and are thought to be heavily
306 involved in familial early-onset obesity in humans[60]. Targeting *mrap2a* with CRISPRa and
307 increasing its transcription would result in a decrease in *mc4r* transcription, which would lead to

308 an increase in larval length. By contrast, silencing *mrap2a* with CRISPRi and decreasing its
309 transcription would lead to an increase in *mc4r* expression, resulting in larvae shorter in length[50,60].
310 While a multitude of loss-of-function experiments have been performed targeting
311 *mrap2a*[50,59,60], gain-of-function (GoF) experiments targeting *mrap2a* have not been explored. As
312 a proof-of-principle experiment, we designed four gRNAs to target the *mrap2a* promoter
313 (Methods) with our CRISPRa system. Zebrafish larvae (n ≥ 200) injected with CRISPRa (300
314 ng/μl) and a cocktail of all *mrap2a* sgRNAs (150 ng/each) displayed marked increase in body
315 length, assayed at 72 hpf (Fig 4A). Similarly, we tested if an individual sgRNA could guide the
316 dCas9-VP64 to modulate body length and found sgRNA3 (150 ng) capable of inducing an
317 observable phenotype (Fig 4A, 4B). By contrast, no increase in larval length was observed at 72
318 hpf in larvae receiving only the CRISPRa mRNA (n ≥ 200) or in uninjected controls (n ≥ 200).
319 Furthermore, we measured the length of larvae receiving CRISPRa+sgRNA3 (n = 50), sgRNA3-
320 only (n = 50), and uninjected controls (n = 50) and performed a Welch two-sample t-test to analyze
321 if the average length between these conditions was statistically different (Fig 4B). At 72 hpf, the
322 average length for these conditions was 3673.67 μm, 3468.86 μm, and 3466.28 μm (p-value =
323 8.58e-16; 1.83e-14, and 0.9181), respectively. The longer larval length phenotype due to
324 increased *mrap2a* transcription and decreased *mc4r* expression is consistent with increased size
325 and weight in mice that become obese due to *mc4r* haploinsufficiency[29], and with morbid obesity
326 cases in humans due to frameshift (loss of function) mutations in *mc4r*[61].
327 We used the same sgRNAs to target and silence *mrap2a* and increase *mc4r* expression.
328 Zebrafish larvae (n ≥ 200) injected with CRISPRi (300 ng/μl) plus all sgRNAs (150 ng/μl/each)
329 displayed a decrease in larval length at 72 hpf (Fig 4A, 4C), which is consistent with rescuing
330 obese mice with *mc4r* haploinsufficiency[29]. Additionally, sgRNA3 was able to guide the dCas9-
331 KRAB-MeCP2 to modulate silencing of *mrap2a* individually and led to a decrease in larval length,
332 observed at 72 hpf (Fig 4A. 4C). By contrast, larval length observed at 72 hpf for larvae receiving
333 only the CRISPRi mRNA (n ≥ 200) or in uninjected controls (n ≥ 200) was higher than our

334 experimental condition (Fig 4A). We also measured the larval length for the conditions
335 CRISPRi+sgRNA3 (n = 50), sgRNA3-only (n = 50), and uninjected controls (n = 50) and found
336 their average length to be 3481.98 μm, 3779.96 μm, and 3748.82 μm, respectively (Fig 4B). We
337 analyzed the statistical significance between these means with a Welch two-sample t-test and
338 found the difference in means between experimental and control conditions to be statistically
339 significant (p-values = 2.2e-16, 2.2e-16, and 0.0636). This further demonstrates that modulating
340 the regulation of one can elicit indirect regulation of other target genes, opening the door to a
341 better understanding gene regulatory networks and their exploration for potential therapeutic
342 interventions.
343

344 DISCUSSION
345

346 CRISPRi/a has emerged as a powerful tool in genetic research, offering the ability to
347 modulate gene expression both for exploration of fundamental mechanisms and for potential
348 therapeutics. It offers the capacity to modulate gene expression without inducing genetic
349 alterations which makes CRISPRi/a an appealing technology for the study of gene regulation and
350 for efficient exploration of both gain and loss of function phenotypes. Nevertheless, its
351 development and application in zebrafish has been slow over the past decade, with only one study
352 describing an effort to implement it[26]., while many others apply CRISPR-based editing
353 technologies[18,19,21,53,54,62].

354 In this study, we chose to fuse a catalytically inactive Cas9 with the transcriptional
355 repressor KRAB-MeCP2. Our choice to use dCas9-KRAB-MeCP2 was guided by previous
356 studies that demonstrated its ability to induce gene silencing while outperforming dCas9-KRAB
357 systems[24,63], implemented in previous CRISPRi experiments in zebrafish[26]. In contrast, for our
358 CRISPRa system, we fused the dCas9 with the transcriptional activator VP64. Comparisons

359 between different Cas9 activators have demonstrated the VP64 to effectively induce gene
360 activation[25]. And while other Cas9 activators such as VPR, SAM, and Suntag have been shown
361 to outperform VP64, these systems have not been tested in zebrafish and/or require special
362 sgRNAs to induce their effect. By using a catalytically inactive Cas9 fused with the transcriptional
363 repressors KRAB-MeCP2 or the transcriptional activator VP64, we have achieved transcriptional
364 control over key genes involved in melanocyte differentiation (*sox10, mitfa, mitfb*), pigmentation
365 (*tyr*), and somatic growth (*mrap2a*) in zebrafish. Our results underscore the versatility and
366 efficiency of CRISPRi/a in zebrafish research. For instance, by silencing *sox10, mitfa, mitfb*, and
367 *tyr*, we successfully were able to obtain zebrafish larvae with marked reduction in pigmentation.
368 Similarly, by activating or silencing *mrap2a*, we successfully modulated larval length.

369 These proof-of-principle experiments underscore the potential of CRISPRi/a technology
370 to control gene expression by targeting gene promoters. CRISIPRi/a is relatively straightforward
371 to implement compared to other genetic editing technologies, which further increases its appeal.
372 In addition, implementing this technology in transparent one-cell zebrafish embryos makes it
373 easier to study the effects of gene silencing and activation during development. Further,
374 CRISPRi/a can also be implemented to study the effects of silencing or activating noncoding
375 regulatory sequences such as enhancers, repressors, and insulators. Taking advantage of the
376 fact that approximately 70% of human genes have a zebrafish gene homolog facilitates the study
377 of gene regulatory mechanisms and networks in yet another vertebrate system. The versatility to
378 study gene expression modulation by either targeting gene promoters or any potential noncoding
379 regulatory sequences in a vertebrate system can offer insights into disease pathogenesis and
380 therapeutic targets that may translate to clinical applications.

381 CRISPRi/a technology, just like CRISPR gene editing, can also be limited by off-target
382 effects and variability in efficiency across genomic loci. Additionally, the ethical implications of
383 gene expression modulation and the potential for unintended consequences underscore the
384 importance of careful consideration in the application of this technology. In this current study, the

primary limitation is the delivery of CRISPRi/a via mRNA microinjections, which is titrated as the embryo develops and the larvae grow older. This results in a diminution of an observable phenotype and hinders the potential to study long-term effects of gene expression modulation, making it difficult to elucidate any potential disease relevance. To this end, we are actively generating stable transgenic lines expressing CRISPRi/a to facilitate rapid and systematic screening of gain or loss of gene function. Our ongoing work will expand the zebrafish toolkit, establishing the utility of CRISPRi/a for evaluation of candidate gene function and disease relevance.

AUTHOR CONTRIBUTIONS: A.S.M., V.C.C, and N.B.B. conceptualized the study. N.B.B. designed codon optimized dCas9-KRAB-MeCP2 and dCas9-VP64 constructs and custom single guide RNAs. N.B.B., E.A.S., and R.J.B. injected RNA constructs into zebrafish embryos. N.B.B. and E.A.S. imaged the fish. N.B.B. and R.J.B. wrote the manuscript. All authors edited and approved the final manuscript for publication.

FUNDING: This research, undertaken at Johns Hopkins University School of Medicine, was supported in part by awards from the National Institutes of Health to A.S.M. (R01HG010480 and R21NS128604), V.C.C. (R35 GM136644), as well as N.B.B., E.A.S., and R.J.B. (T32 GM007814-40); and by the Canadian Institutes of Health Research (DFD-181599) to R.J.B.

DATA AVAILABILITY: N/A

ACKNOWLEDGEMENTS: The authors would like to acknowledge the FInZ Zebrafish Core Center for assistance with zebrafish husbandry.

CONFLICTS OF INTEREST: The authors declare no competing interests.

411

412 REFERENCES

413

414 1. Giffen, K.P., Liu, H., Kramer, K.L., and He, D.Z. (2019). Expression of Protein-Coding
415 Gene Orthologs in Zebrafish and Mouse Inner Ear Non-sensory Supporting Cells. Front
416 Neurosci *13*. https://doi.org/10.3389/FNINS.2019.01117/FULL.

417 2. Howe, K., Clark, M.D., Torroja, C.F., Torrance, J., Berthelot, C., Muffato, M., Collins, J.E.,
418 Humphray, S., McLaren, K., Matthews, L., et al. (2013). The zebrafish reference genome
419 sequence and its relationship to the human genome. Nature *496*, 498–503.
420 https://doi.org/10.1038/NATURE12111.

421 3. Fisher, S., Grice, E.A., Vinton, R.M., Bessling, S.L., Urasaki, A., Kawakami, K., and
422 McCallion, A.S. (2006). Evaluating the biological relevance of putative enhancers using
423 Tol2 transposon-mediated transgenesis in zebrafish. Nature Protocols 2006 1:3 *1*, 1297–
424 1305. https://doi.org/10.1038/nprot.2006.230.

425 4. Gorkin, D.U., Lee, D., Reed, X., Fletez-Brant, C., Bessling, S.L., Loftus, S.K., Beer, M.A.,
426 Pavan, W.J., and McCallion, A.S. (2012). Integration of ChIP-seq and machine learning
427 reveals enhancers and a predictive regulatory sequence vocabulary in melanocytes.
428 Genome Res *22*, 2290–2301. https://doi.org/10.1101/GR.139360.112.

429 5. Fisher, S., Grice, E.A., Vinton, R.M., Bessling, S.L., and McCallion, A.S. (2006).
430 Conservation of RET regulatory function from human to zebrafish without sequence
431 similarity. Science *312*, 276–279. https://doi.org/10.1126/SCIENCE.1124070.

432 6. Antonellis, A., Huynh, J.L., Lee-Lin, S.Q., Vinton, R.M., Renaud, G., Loftus, S.K., Elliot,
433 G., Wolfsberg, T.G., Green, E.D., McCallion, A.S., et al. (2008). Identification of neural
434 crest and glial enhancers at the mouse Sox10 locus through transgenesis in zebrafish.
435 PLoS Genet *4*. https://doi.org/10.1371/JOURNAL.PGEN.1000174.

436 7. Doyle, A.J., Doyle, J.J., Bessling, S.L., Maragh, S., Lindsay, M.E., Schepers, D., Gillis, E.,
437 Mortier, G., Homfray, T., Sauls, K., et al. (2012). Mutations in the TGF-β repressor SKI
438 cause Shprintzen-Goldberg syndrome with aortic aneurysm. Nat Genet *44*, 1249–1254.
439 https://doi.org/10.1038/NG.2421.

440 8. Gould, R.A., Aziz, H., Woods, C.E., Seman-Senderos, M.A., Sparks, E., Preuss, C.,
441 Wünnemann, F., Bedja, D., Moats, C.R., McClymont, S.A., et al. (2019). ROBO4 variants
442 predispose individuals to bicuspid aortic valve and thoracic aortic aneurysm. Nat Genet
443 *51*, 42–50. https://doi.org/10.1038/S41588-018-0265-Y.

444 9. Golzio, C., Willer, J., Talkowski, M.E., Oh, E.C., Taniguchi, Y., Jacquemont, S.,
445 Reymond, A., Sun, M., Sawa, A., Gusella, J.F., et al. (2012). KCTD13 is a major driver of
446 mirrored neuroanatomical phenotypes of the 16p11.2 copy number variant. Nature *485*,
447 363–367. https://doi.org/10.1038/NATURE11091.

448 10. Panizzi, J.R., Becker-Heck, A., Castleman, V.H., Al-Mutairi, D.A., Liu, Y., Loges, N.T.,
449 Pathak, N., Austin-Tse, C., Sheridan, E., Schmidts, M., et al. (2012). CCDC103 mutations

450 cause primary ciliary dyskinesia by disrupting assembly of ciliary dynein arms. Nat Genet
451 *44*, 714–719. https://doi.org/10.1038/NG.2277.

452 11. Roscioli, T., Kamsteeg, E.J., Buysse, K., Maystadt, I., Van Reeuwijk, J., Van Den Elzen,
453 C., Van Beusekom, E., Riemersma, M., Pfundt, R., Vissers, L.E.L.M., et al. (2012).
454 Mutations in ISPD cause Walker-Warburg syndrome and defective glycosylation of α-
455 dystroglycan. Nat Genet *44*, 581–585. https://doi.org/10.1038/NG.2253.

456 12. Tobin, D.M., Roca, F.J., Oh, S.F., McFarland, R., Vickery, T.W., Ray, J.P., Ko, D.C., Zou,
457 Y., Bang, N.D., Chau, T.T.H., et al. (2012). Host genotype-specific therapies can optimize
458 the inflammatory response to mycobacterial infections. Cell *148*, 434–446.
459 https://doi.org/10.1016/J.CELL.2011.12.023.

460 13. Maragh, S., Miller, R.A., Bessling, S.L., McGaughey, D.M., Wessels, M.W., De Graaf, B.,
461 Stone, E.A., Bertoli-Avella, A.M., Gearhart, J.D., Fisher, S., et al. (2011). Identification of
462 RNA binding motif proteins essential for cardiovascular development. BMC Dev Biol *11*.
463 https://doi.org/10.1186/1471-213X-11-62.

464 14. Wahbeh, M.H., Boyd, R.J., Yovo, C., Rike, B., McCallion, A.S., and Avramopoulos, D.
465 (2024). A functional schizophrenia-associated genetic variant near the TSNARE1 and
466 ADGRB1 genes. HGG Adv *5*. https://doi.org/10.1016/J.XHGG.2024.100303.

467 15. Asakawa, K., and Kawakami, K. (2008). Targeted gene expression by the Gal4-UAS
468 system in zebrafish. Dev Growth Differ *50*, 391–399. https://doi.org/10.1111/J.1440-
469 169X.2008.01044.X.

470 16. Zhu, C., Smith, T., Mcnulty, J., Rayla, A.L., Lakshmanan, A., Siekmann, A.F., Buffardi,
471 M., Meng, X., Shin, J., Padmanabhan, A., et al. (2011). Evaluation and application of
472 modularly assembled zinc-finger nucleases in zebrafish. Development *138*, 4555–4564.
473 https://doi.org/10.1242/DEV.066779.

474 17. Huang, P., Xiao, A., Zhou, M., Zhu, Z., Lin, S., and Zhang, B. (2011). Heritable gene
475 targeting in zebrafish using customized TALENs. Nature Biotechnology 2011 29:8 *29*,
476 699–700. https://doi.org/10.1038/nbt.1939.

477 18. Hwang, W.Y., Fu, Y., Reyon, D., Maeder, M.L., Tsai, S.Q., Sander, J.D., Peterson, R.T.,
478 Yeh, J.R.J., and Joung, J.K. (2013). Efficient genome editing in zebrafish using a
479 CRISPR-Cas system. Nat Biotechnol *31*, 227–229. https://doi.org/10.1038/NBT.2501.

480 19. Shah, A.N., Davey, C.F., Whitebirch, A.C., Miller, A.C., and Moens, C.B. (2015). Rapid
481 reverse genetic screening using CRISPR in zebrafish. Nat Methods *12*, 535–540.
482 https://doi.org/10.1038/NMETH.3360.

483 20. Varshney, G.K., Pei, W., Lafave, M.C., Idol, J., Xu, L., Gallardo, V., Carrington, B.,
484 Bishop, K., Jones, M., Li, M., et al. (2015). High-throughput gene targeting and
485 phenotyping in zebrafish using CRISPR/Cas9. Genome Res *25*, 1030–1042.
486 https://doi.org/10.1101/GR.186379.114.

487 21. Zhang, Y., Qin, W., Lu, X., Xu, J., Huang, H., Bai, H., Li, S., and Lin, S. (2017).
488 Programmable base editing of zebrafish genome using a modified CRISPR-Cas9 system.
489 Nat Commun *8*. https://doi.org/10.1038/S41467-017-00175-6.

490 22. Hisano, Y., Sakuma, T., Nakade, S., Ohga, R., Ota, S., Okamoto, H., Yamamoto, T., and
491 Kawahara, A. (2015). Precise in-frame integration of exogenous DNA mediated by
492 CRISPR/Cas9 system in zebrafish. Sci Rep *5*. https://doi.org/10.1038/SREP08841.

493 23. Larson, M.H., Gilbert, L.A., Wang, X., Lim, W.A., Weissman, J.S., and Qi, L.S. (2013).
494 CRISPR interference (CRISPRi) for sequence-specific control of gene expression. Nature
495 Protocols 2013 8:11 *8*, 2180–2196. https://doi.org/10.1038/nprot.2013.132.

496 24. Yeo, N.C., Chavez, A., Lance-Byrne, A., Chan, Y., Menn, D., Milanova, D., Kuo, C.C.,
497 Guo, X., Sharma, S., Tung, A., et al. (2018). An enhanced CRISPR repressor for targeted
498 mammalian gene regulation. Nat Methods *15*, 611–616. https://doi.org/10.1038/S41592-
499 018-0048-5.

500 25. Chavez, A., Tuttle, M., Pruitt, B.W., Ewen-Campen, B., Chari, R., Ter-Ovanesyan, D.,
501 Haque, S.J., Cecchi, R.J., Kowal, E.J.K., Buchthal, J., et al. (2016). Comparison of Cas9
502 activators in multiple species. Nat Methods *13*, 563–567.
503 https://doi.org/10.1038/NMETH.3871.

504 26. Long, L., Guo, H., Yao, D., Xiong, K., Li, Y., Liu, P., Zhu, Z., and Liu, D. (2015).
505 Regulation of transcriptionally active genes via the catalytically inactive Cas9 in C.
506 elegans and D. rerio. Cell Research 2015 25:5 *25*, 638–641.
507 https://doi.org/10.1038/cr.2015.35.

508 27. Sastre, D., Zafar, F., Torres, C.A.M., Piper, D., Kirik, D., Sanders, L.H., Qi, L.S., and
509 Schüle, B. (2023). Inactive S. aureus Cas9 downregulates alpha-synuclein and reduces
510 mtDNA damage and oxidative stress levels in human stem cell model of Parkinson's
511 disease. Sci Rep *13*. https://doi.org/10.1038/S41598-023-45078-3.

512 28. Matharu, N., and Ahituv, N. (2020). Modulating gene regulation to treat genetic disorders.
513 Nature Reviews Drug Discovery 2020 19:11 *19*, 757–775.
514 https://doi.org/10.1038/s41573-020-0083-7.

515 29. Matharu, N., Rattanasopha, S., Tamura, S., Maliskova, L., Wang, Y., Bernard, A., Hardin,
516 A., Eckalbar, W.L., Vaisse, C., and Ahituv, N. (2019). CRISPR-mediated activation of a
517 promoter or enhancer rescues obesity caused by haploinsufficiency. Science (1979) *363*.
518 https://doi.org/10.1126/SCIENCE.AAU0629/SUPPL_FILE/AAU0629_TABLE_S6.XLSX.

519 30. Camp, E., and Lardelli, M. (2001). Tyrosinase gene expression in zebrafish embryos. Dev
520 Genes Evol *211*, 150–153. https://doi.org/10.1007/S004270000125/METRICS.

521 31. Cooper, C.D., and Raible, D.W. (2009). Mechanisms for reaching the differentiated state:
522 Insights from neural crest-derived melanocytes. Semin Cell Dev Biol *20*, 105–110.
523 https://doi.org/10.1016/J.SEMCDB.2008.09.008.

524 32. Haffter, P., Odenthal, J., Mullins, M.C., Lin, S., Farrell, M.J., Vogelsang, E., Haas, F.,
525 Brand, M., Van Eeden, F.J.M., Furutani-Seiki, M., et al. (1996). Mutations affecting
526 pigmentation and shape of the adult zebrafish. Dev Genes Evol *206*, 260–276.
527 https://doi.org/10.1007/S004270050051/METRICS.

528 33. Lane, B.M., and Lister, J.A. (2012). Otx but Not Mitf Transcription Factors Are Required
529 for Zebrafish Retinal Pigment Epithelium Development. PLoS One *7*, 49357.
530 https://doi.org/10.1371/JOURNAL.PONE.0049357.

531 34. Lister, J.A., Close, J., and Raible, D.W. (2001). Duplicate mitf genes in zebrafish:
532 complementary expression and conservation of melanogenic potential. Dev Biol *237*,
533 333–344. https://doi.org/10.1006/DBIO.2001.0379.

534 35. Murisier, F., Guichard, S., and Beermann, F. (2007). The tyrosinase enhancer is
535 activated by Sox10 and Mitf in mouse melanocytes. Pigment Cell Res *20*, 173–184.
536 https://doi.org/10.1111/J.1600-0749.2007.00368.X.

537 36. Dutton, K.A., Pauliny, A., Lopes, S.S., Elworthy, S., Carney, T.J., Rauch, J., Geisler, R.,
538 Haffter, P., and Kelsh, R.N. (2001). Zebrafish colourless encodes sox10 and specifies
539 non-ectomesenchymal neural crest fates. Development *128*, 4113–4125.
540 https://doi.org/10.1242/DEV.128.21.4113.

541 37. Johnson, S.L., Nguyen, A.T.N., and Lister, J.A. (2011). mitfa is required at multiple stages
542 of melanocyte differentiation but not to establish the melanocyte stem cell. Dev Biol *350*,
543 405. https://doi.org/10.1016/J.YDBIO.2010.12.004.

544 38. Wang, C., Kocher, T.D., Wu, J., Li, P., Liang, G., Lu, B., Xu, J., Chen, X., and Wang, D.
545 (2023). Knockout of microphthalmia-associated transcription factor (mitf) confers a red
546 and yellow tilapia with few pigmented melanophores. Aquaculture *565*, 739151.
547 https://doi.org/10.1016/J.AQUACULTURE.2022.739151.

548 39. Wu, Y.C., and Wang, I.J. (2020). Heat-shock-induced tyrosinase gene ablation with
549 CRISPR in zebrafish. Molecular Genetics and Genomics *295*, 911–922.
550 https://doi.org/10.1007/S00438-020-01681-X/FIGURES/6.

551 40. Camp, E., Badhwar, P., Mann, G.J., and Lardelli, M. (2003). Expression Analysis of a
552 Tyrosinase Promoter Sequence in Zebrafish. Pigment Cell Res *16*, 117–126.
553 https://doi.org/10.1034/J.1600-0749.2003.00002.X.

554 41. Frantz, W.T., and Ceol, C.J. (2020). From Tank to Treatment: Modeling Melanoma in
555 Zebrafish. Cells *9*. https://doi.org/10.3390/CELLS9051289.

556 42. Praetorius, C., Grill, C., Stacey, S.N., Metcalf, A.M., Gorkin, D.U., Robinson, K.C., Van
557 Otterloo, E., Kim, R.S.Q., Bergsteinsdottir, K., Ogmundsdottir, M.H., et al. (2013). A
558 polymorphism in IRF4 affects human pigmentation through a tyrosinase-dependent
559 MITF/TFAP2A pathway. Cell *155*, 1022. https://doi.org/10.1016/J.CELL.2013.10.022.

560 43. Rosenbaum, S.R., Tiago, M., Caksa, S., Capparelli, C., Purwin, T.J., Kumar, G.,
561 Glasheen, M., Pomante, D., Kotas, D., Chervoneva, I., et al. (2021). SOX10 requirement
562 for melanoma tumor growth is due, in part, to immune-mediated effects. Cell Rep *37*.
563 https://doi.org/10.1016/J.CELREP.2021.110085.

564 44. Gudbjartsson, D.F., Sulem, P., Stacey, S.N., Goldstein, A.M., Rafnar, T., Sigurgeirsson,
565 B., Benediktsdottir, K.R., Thorisdottir, K., Ragnarsson, R., Sveinsdottir, S.G., et al.
566 (2008). ASIP and TYR pigmentation variants associate with cutaneous melanoma and
567 basal cell carcinoma. Nat Genet *40*, 886–891. https://doi.org/10.1038/NG.161.

568 45. Garraway, L.A., Widlund, H.R., Rubin, M.A., Getz, G., Berger, A.J., Ramaswamy, S.,
569 Beroukhim, R., Milner, D.A., Granter, S.R., Du, J., et al. (2005). Integrative genomic
570 analyses identify MITF as a lineage survival oncogene amplified in malignant melanoma.
571 Nature *436*, 117–122. https://doi.org/10.1038/NATURE03664.

572 46. Tassabehji, M., Newton, V.E., and Read, A.P. (1994). Waardenburg syndrome type 2
573 caused by mutations in the human microphthalmia (MITF) gene. Nat Genet *8*, 251–255.
574 https://doi.org/10.1038/NG1194-251.

575 47. Bondurand, N., Pingault, V., Goerich, D.E., Lemort, N., Sock, E., Le Caignec, C.,
576 Wegner, M., and Goossens, M. (2000). Interaction among SOX10, PAX3 and MITF, three
577 genes altered in Waardenburg syndrome. Hum Mol Genet *9*, 1907–1917.
578 https://doi.org/10.1093/HMG/9.13.1907.

579 48. Paratore, C., Eichenberger, C., Suter, U., and Sommer, L. (2002). Sox10
580 haploinsufficiency affects maintenance of progenitor cells in a mouse model of
581 Hirschsprung disease. Hum Mol Genet *11*, 3075–3085.
582 https://doi.org/10.1093/HMG/11.24.3075.

583 49. Mccallion, A.S., and Chakravarti, A. (2001). EDNRB/EDN3 and Hirschsprung disease
584 type II. Pigment Cell Res *14*, 161–169. https://doi.org/10.1034/J.1600-
585 0749.2001.140305.X.

586 50. Sebag, J.A., Zhang, C., Hinkle, P.M., Bradshaw, A.M., and Cone, R.D. (2013).
587 Developmental Control of the Melanocortin-4 Receptor by MRAP2 Proteins in Zebrafish.
588 Science *341*, 278. https://doi.org/10.1126/SCIENCE.1232995.

589 51. Yeo, G.S.H., Farooqi, I.S., Aminian, S., Halsall, D.J., Stanhope, R.G., and O'Rahilly, S.
590 (1998). A frameshift mutation in MC4R associated with dominantly inherited human
591 obesity. Nat Genet *20*, 111–112. https://doi.org/10.1038/2404.

592 52. Wade, K.H., Lam, B.Y.H., Melvin, A., Pan, W., Corbin, L.J., Hughes, D.A., Rainbow, K.,
593 Chen, J.H., Duckett, K., Liu, X., et al. (2021). Loss-of-function mutations in the
594 melanocortin 4 receptor in a UK birth cohort. Nat Med *27*, 1088–1096.
595 https://doi.org/10.1038/S41591-021-01349-Y.

596 53. Amorim, J.P., Bordeira-Carriço, R., Gali-Macedo, A., Perrod, C., and Bessa, J. (2020).
597 CRISPR-Cas9-Mediated Genomic Deletions Protocol in Zebrafish. STAR Protoc *1*.
598 https://doi.org/10.1016/J.XPRO.2020.100208.

599 54. Jao, L.E., Wente, S.R., and Chen, W. (2013). Efficient multiplex biallelic zebrafish
600 genome editing using a CRISPR nuclease system. Proc Natl Acad Sci U S A *110*,
601 13904–13909. https://doi.org/10.1073/PNAS.1308335110.

602 55. Kawakami, A., and Fisher, D.E. (2017). The master role of microphthalmia-associated
603 transcription factor in melanocyte and melanoma biology. Laboratory Investigation 2017
604 97:6 *97*, 649–656. https://doi.org/10.1038/labinvest.2017.9.

605 56. Cooper, C.D. (2017). Insights from zebrafish on human pigment cell disease and
606 treatment. Developmental Dynamics *246*, 889–896. https://doi.org/10.1002/DVDY.24550.

607 57. Moreno-Marmol, T., Cavodeassi, F., and Bovolenta, P. (2018). Setting eyes on the retinal
608 pigment epithelium. Front Cell Dev Biol *6*, 418922.
609 https://doi.org/10.3389/FCELL.2018.00145/BIBTEX.

610 58. Cunningham, R.L., Kramer, E.T., DeGeorgia, S.K., Godoy, P.M., Zarov, A.P.,
611 Seneviratne, S., Grigura, V., and Kaufman, C.K. (2021). Functional in vivo

612 characterization of sox10 enhancers in neural crest and melanoma development.
613 Communications Biology 2021 4:1 *4*, 1–15. https://doi.org/10.1038/s42003-021-02211-0.

614 59. Baron, M., Maillet, J., Huyvaert, M., Dechaume, A., Boutry, R., Loiselle, H., Durand, E.,
615 Toussaint, B., Vaillant, E., Philippe, J., et al. (2019). Loss-of-function mutations in MRAP2
616 are pathogenic in hyperphagic obesity with hyperglycemia and hypertension. Nature
617 Medicine 2019 25:11 *25*, 1733–1738. https://doi.org/10.1038/s41591-019-0622-0.

618 60. Asai, M., Ramachandrappa, S., Joachim, M., Shen, Y., Zhang, R., Nuthalapati, N.,
619 Ramanathan, V., Strochlic, D.E., Ferket, P., Linhart, K., et al. (2013). Loss of function of
620 the melanocortin 2 receptor accessory protein 2 is associated with mammalian obesity.
621 Science (1979) *341*, 275–278.
622 https://doi.org/10.1126/SCIENCE.1233000/SUPPL_FILE/ASAI-SM.PDF.

623 61. Vaisse, C., Clement, K., Durand, E., Hercberg, S., Guy-Grand, B., and Froguel, P.
624 (2000). Melanocortin-4 receptor mutations are a frequent and heterogeneous cause of
625 morbid obesity. J Clin Invest *106*, 253–262. https://doi.org/10.1172/JCI9238.

626 62. de Vrieze, E., de Bruijn, S.E., Reurink, J., Broekman, S., van de Riet, V., Aben, M.,
627 Kremer, H., and van Wijk, E. (2021). Efficient generation of knock-in zebrafish models for
628 inherited disorders using crispr-cas9 ribonucleoprotein complexes. Int J Mol Sci *22*, 9429.
629 https://doi.org/10.3390/IJMS22179429/S1.

630 63. Alerasool, N., Segal, D., Lee, H., and Taipale, M. (2020). An efficient KRAB domain for
631 CRISPRi applications in human cells. Nature Methods 2020 17:11 *17*, 1093–1096.
632 https://doi.org/10.1038/s41592-020-0966-x.

633

634

635

636 FIGURES

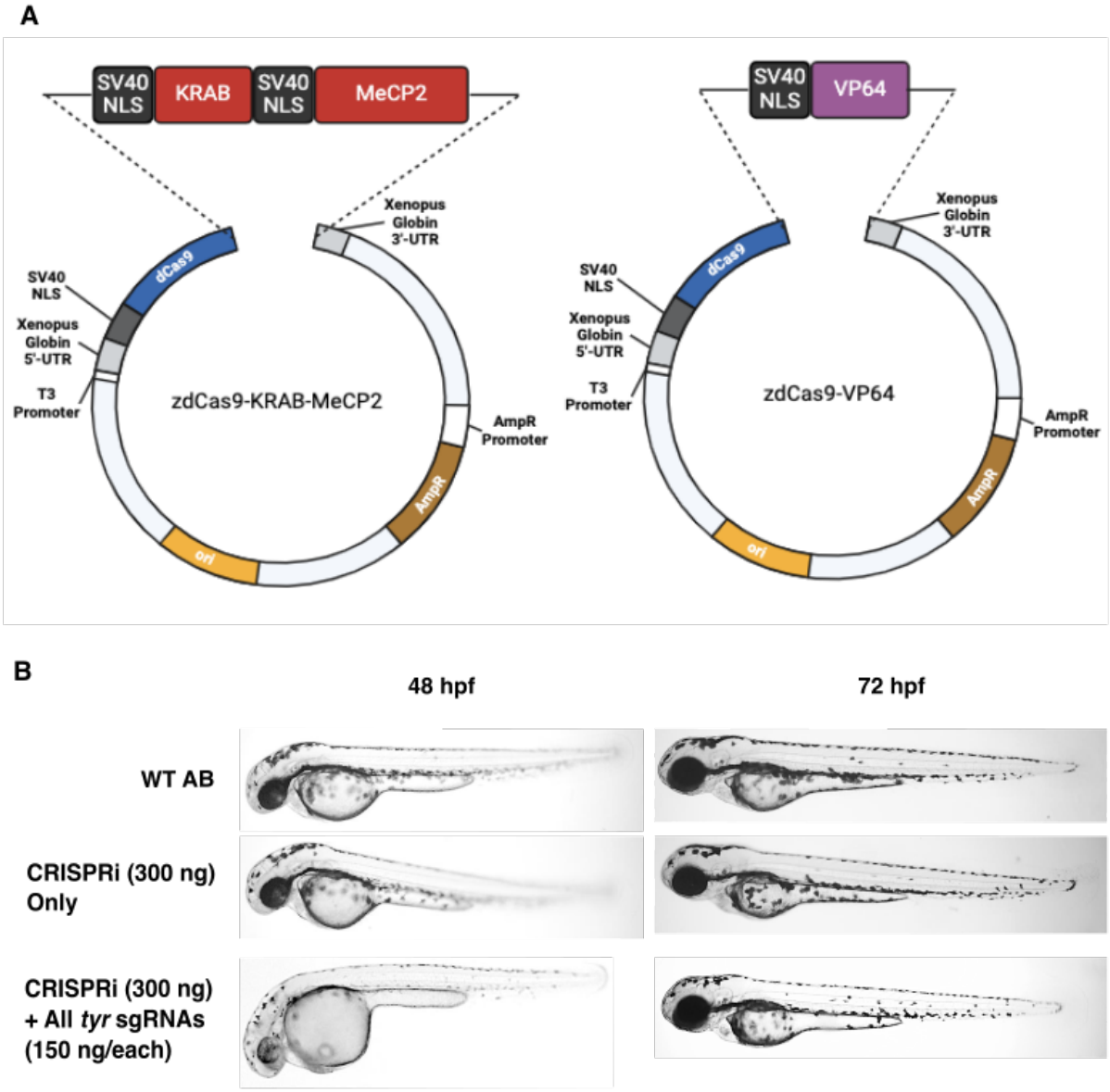

637

638 ***Figure 1:*** CRISPRi/a construct design. **A.** Zebrafish codon-optimized plasmids were linearized and *in vitro*
639 transcribed before microinjection into one-cell embryos. **B.** Zebrafish embryos injected with CRISPRi +
640 sgRNAs targeting *tyr* assayed at 48 and 78 hpf for differences in pigmentation patterns. Larvae injected
641 with CRISPRi and sgRNAs displayed reduced pigmentation at 48 hpf when compared to controls. The
642 effect of CRISPRi dissipated by 72 hpf as observable pigmentation patterns where indistinguishable.

643

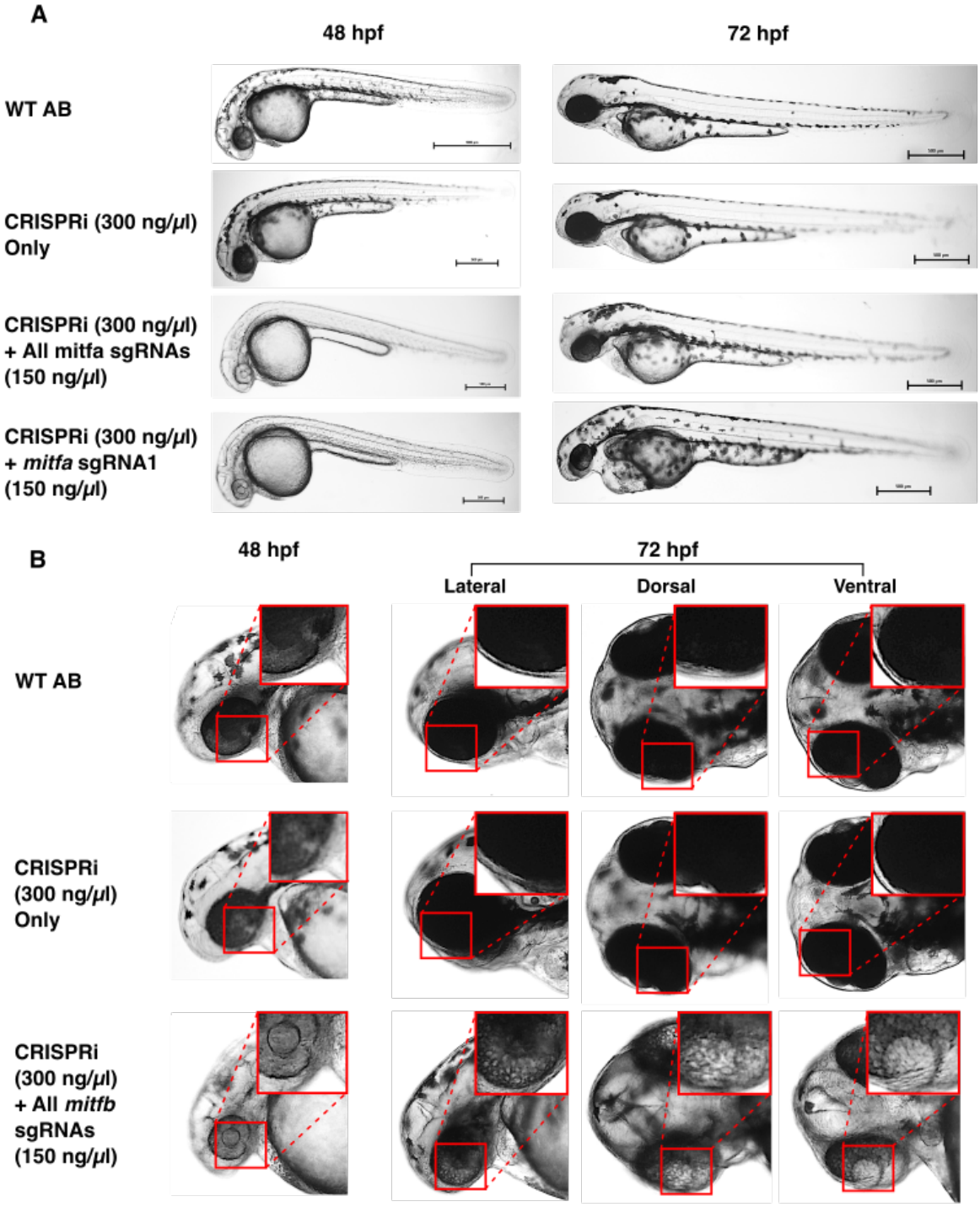

Figure 2: CRISPRi targeting *mitf* genes. **A.** Zebrafish embryos injected with CRISPRi + sgRNAs targeting *mitfa* assayed at 48 and 72 hpf for differences in pigmentation patterns. WT AB and injected controls did not show reduced pigmentation at 48 hpf, whereas embryos injected with all sgRNAs or only sgRNA1 (targets 5'-UTR) displayed the hypopigmentation phenotype at 48 hpf. The effect of CRISPRi dissipated by 72 hpf as patterns of hypopigmentation were not observed between conditions. Scale bars: 500 or 1000 μm. **B.** Zebrafish embryos injected with CRISPRi + sgRNAs targeting *mitfb* assayed at 48 and 72 hpf for

differences in pigmentation patterns in the RPE. Among conditions, the RPE was not fully pigmented at 48 hpf, with further delayed pigmentation in larvae injected with CRISPRi + sgRNAs. At 72 hpf, the RPE was fully pigmented among controls but not in the experimental condition as seen laterally, dorsally, and ventrally.

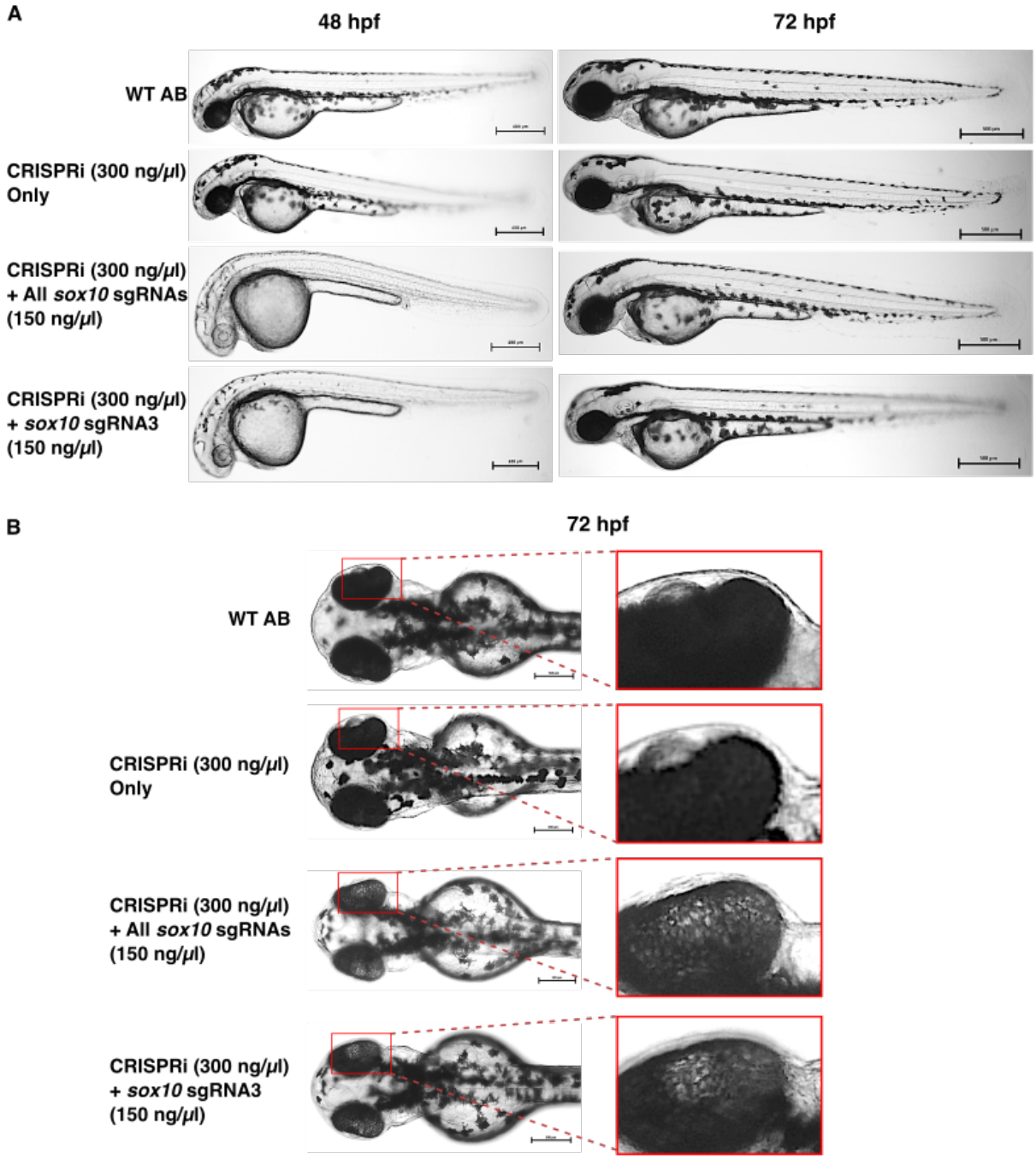

Figure 3: CRISPRi targeting the *sox10* gene. **A.** Zebrafish embryos injected with CRISPRi + sgRNAs targeting *sox10* assayed at 48 and 72 hpf for differences in pigmentation patterns. WT AB and injected controls did not show reduced pigmentation at 48 hpf, whereas embryos injected with all sgRNAs or only sgRNA3 were hypopigmented and delayed in development. The effect of CRISPRi dissipated by 72 hpf as patterns of hypopigmentation were not observed between conditions. Scale bars: 600 µm. **B.** Silencing *sox10* creates patches of hypopigmentation in the RPE at 72 hpf. The RPE in controls is fully pigmented at 72 hpf. Scale bars 600 µm.

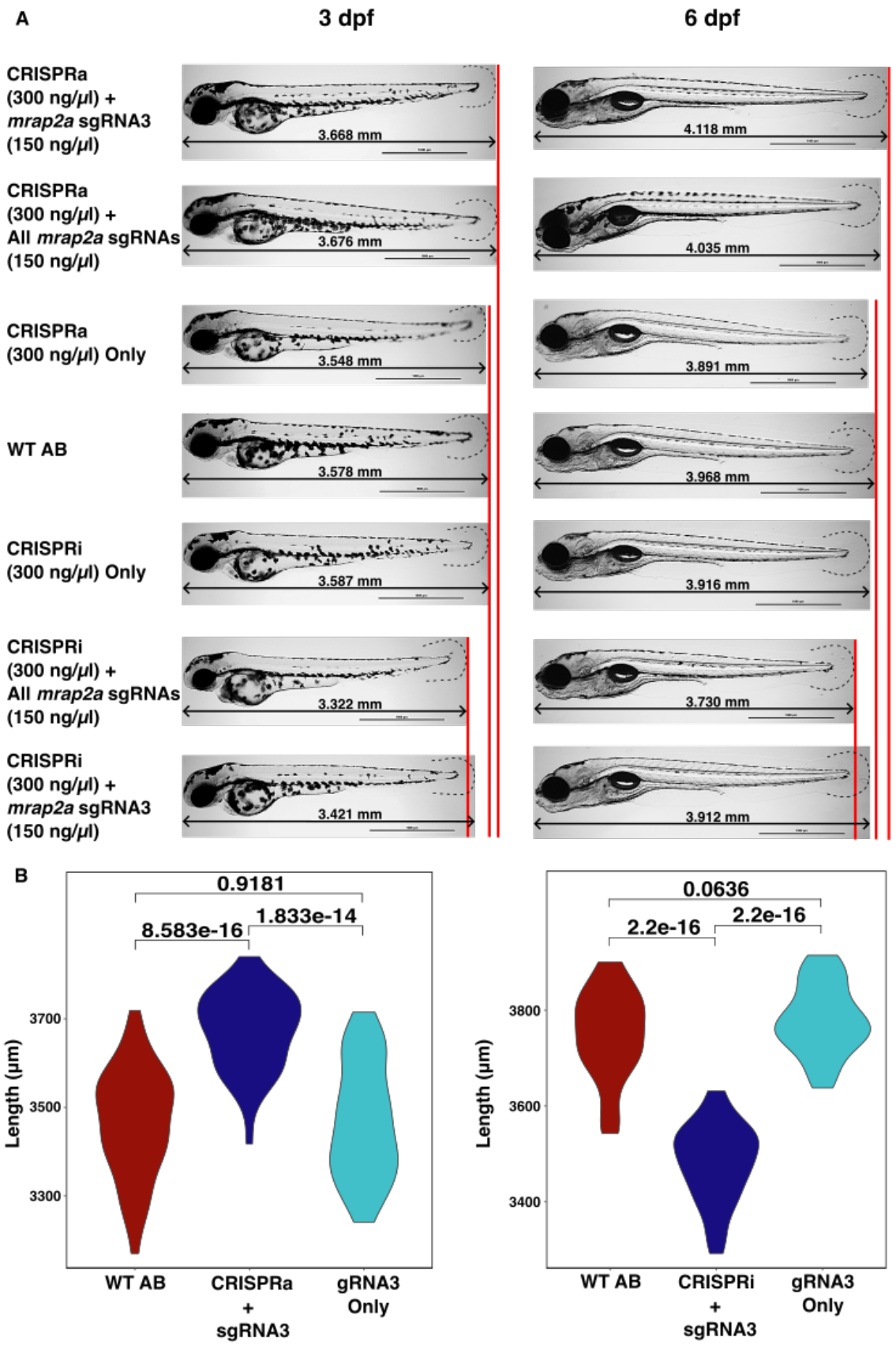
A
3 dpf
6 dpf
CRISPRa (300 ng/μl) + mrap2a sgRNA3 (150 ng/μl)
3.668 mm
4.118 mm
CRISPRa (300 ng/μl) + All mrap2a sgRNAs (150 ng/μl)
3.676 mm
4.035 mm
CRISPRa (300 ng/μl) Only
3.548 mm
3.891 mm
WT AB
3.578 mm
3.968 mm
CRISPRi (300 ng/μl) Only
3.587 mm
3.916 mm
CRISPRi (300 ng/μl) + All mrap2a sgRNAs (150 ng/μl)
3.322 mm
3.730 mm
CRISPRi (300 ng/μl) + mrap2a sgRNA3 (150 ng/μl)
3.421 mm
3.912 mm
B
0.9181
8.583e-16
1.833e-14
Length (μm)
3700
3500
3300
WT AB
CRISPRa + sgRNA3
gRNA3 Only
0.0636
2.2e-16
2.2e-16
Length (μm)
3800
3600
3400
WT AB
CRISPRi + sgRNA3
gRNA3 Only

664

665 ***Figure 4:*** Targeting *mrap2a* with CRISPRa and CRISPRi. **A.** Length comparison at 3 and 6 dpf between
666 WT AB embryos and embryos injected with CRISPRa and CRISPRi. Length measured laterally from tip of
667 the head to end of fin tail (dashed lines). Red lines depict length differences between controls and
668 experimental conditions. Scale bars: 1000 μm. **B.** At 3 dpf, 50 larvae per condition were measured in
669 length and compared. The Welch two-sample t-test was used to compare the average length between
670 conditions.

671